5-2019

Development of a Serological Diagnostic assay for *Elaeophora schneideri* infection in moose (*Alces alces*)

Megan D. Miller
University of Tennessee

Development of a Serological Diagnostic assay for *Elaeophora schneideri* infection in moose (*Alces alces)*

A Thesis Presented for the

Master of Science

Degree

The University of Tennessee, Knoxville

Megan D. Miller

May 2019

DEDICATION

To the UTCVM anatomic pathologists and residents who made my afternoons so delightfully gross.

ACKNOWLEDGEMENTS

First and foremost, I would like to acknowledge the Comparative and Experimental Medicine program at the University of Tennessee for providing guidance and my living stipend. I would also like to express my utmost gratitude to Jessie Richards, who taught me everything I know and kept me sane through a lot of frustrating weeks and months. My utmost appreciation goes to Nicholas DeCesare and Montana Fish, Wildlife, & Parks for his moose expertise and for providing many of the *Elaeophora schneideri* nematode samples used in this thesis. I thank Utah Department of Natural Resources, Minnesota Department of Natural Resources, Alaska Department of Fish and Game, and Washington Department of Fish and Wildlife for their financial and experimental support.

ABSTRACT

Elaeophora schneideri is a nematode which inhabits the arteries of its domestic and free-ranging ungulate hosts. It is the etiological agent of elaeophorosis, a proven cause of morbidity and mortality in ungulates, including moose. Moose numbers are declining in several U.S. states and Canadian provinces, and recent research suggests that *Elaeophora schneideri* is a factor in these declines. At this time, the only conclusive method for diagnosing elaeophorosis requires finding nematodes or arterial lesions in recently deceased moose. The lack of a serological diagnostic test has made the prevalence, significance, and geographical distribution of this parasite difficult to assess. This research is an investigation of antigenic potential of *E. schneideri* proteins. Ultimately, these proteins will be utilized in developing an enzyme-linked immunosorbent assay (ELISA) to detect anti-*Elaeophora* antibodies in moose sera. Genome sequencing and transcriptome analysis were effective in identifying two genes encoding peptides that are predicted to be immunogenic.

We prepared the synthetic genes encoding these peptides and used them to transform TOPO-brand *E. coli* cells (Invitrogen, Carlsbad, California). Despite successful transformation and culturing in LB Broth with 0.05 % [percent] ampicillin, attempts to isolate the polyhistidine-tagged proteins were unsuccessful. However, one western blot did result in distinct bands when probed with 6x anti-histidine monoclonal antibody. One of these bands was the approximate weight of the smaller of the two recombinant proteins (8.94 kDa); this band also appeared when the blot was probed with *E. schneideri*-positive moose serum, but did not appear when probed with *E. schneideri*-negative deer serum. This result was unable to be replicated, but may indicate this protein is a useful antigen. Future research will utilize sub-cloning procedures to insert PCR-amplified synthetic, optimized genes into pETBlue-2 cells. This should produce effective recombinant proteins which can be isolated using the his-tags on the proteins. These proteins will be able to be used in an ELISA to detect current or previous *E. schneideri* infection in moose.

TABLE OF CONTENTS

LIST OF FIGURES

PREFACE

Elaeophora schneideri was first described in 1935 in a domestic sheep (Wehr and Dikmans 1935). At this time, *E. schneideri* research focused primarily on livestock. After the initial description and research, inquiries about this parasite would remain quiet until the 1960s, when Charles Hibler and J. L. Adcock began to explore its role in wildlife. They studied the topic extensively through basic research and experimental infections of both domestic and free-ranging animals, and their research is the foundation of our current knowledge of the parasite. However, research into *E. schneideri* slowed considerably over the next several decades. From the mid-1980s to the early-2010s, a paper would come out every year or two. However, in 2012, wildlife researchers published their observations on prevalence of *E. schneideri* in moose and its correlation with moose (*Alces alces)* declines in North America.

Further study of *Elaeophora schneideri* with modern technologies has been complicated -- at this time, diagnosis of infection with this parasite is not possible prior to the death of the host. Without an accurate diagnostic test, very little data has been generated on the prevalence, distribution, and impact of this parasite on moose populations. Given the potential impact of this parasite on declining moose population, there is an urgent need for a simple and definitive antemortem diagnostic test for *E. schneideri*.

The research set forth by this thesis aims to address the issue posed by the lack of a diagnostic test for *Elaeophora schneideri* infection in moose. The methods herein may also be used to develop diagnostic tests for nematode infections in other cervid species in the future.

CHAPTER I
LITERATURE REVIEW

Moose in North America

Moose (*Alces alces*) are the largest living member of the Cervidae family which includes elk (*Cervus canadensis*), caribou (*Rangifer tarandus*), sambar (*Rusa unicolor*), and white-tailed deer (*Odocoileus virginianus*). There are eight extant subspecies of moose, four of which reside in North America: *Alces alces gigas, Alces alces andersoni, Alces alces americana,* and *Alces alces shirasi* (Clinton, 1822; Miller, 1899; Nelson, 1914; Peterson, 1952; Peterson, 1955). Their range includes boreal forests, temperate broadleaf forests, and mixed forest in temperate to subarctic climates of North America. In the United States, they occupy regions of northern New England, northern New York, Minnesota, northern Michigan, Wyoming, North Dakota, Montana, Colorado, Utah, Idaho, Oregon, Washington, and Alaska.

Moose are strict herbivores, primarily consuming woody plants and leaves by browsing (Kie, 1999). In the spring and summer, they consume fresh tree shoots, forbs, and other non-grasses (Miquelle, 1983); in colder weather, they feed primarily on twigs and other woody vegetation such as aspen (*Populus* spp.) shoots (Dannell et al., 1991). When climate permits, moose consume aquatic vegetation to fulfil their sodium requirements (Belovsky and Jordan, 1981).

Moose are sexually dimorphic, with adult males being larger than adult females (Bubenik, 2007). Adult males display a large set of palmate antlers which are thought to be used for fighting and defense against other male moose (Clutton-Brock and Albon, 1980; Clutton-Brock, 1982) or as parabolic reflectors of sound into their ears (Bubenik and Bubenik, 2008). Female moose do not grow antlers. Moose are mostly solitary (Peek et al. 1974; Testa, 2004). In general, moose only interact with other moose to mate (Cederlund and Sand, 1994). Two to three moose may be observed together, though these are usually a cow and her single or twin offspring (Matthews, 2012; Peek et al., 1974).

Moose have a considerable effect on the ecosystem, primarily through browsing activity (Sinclair, 2003; Bergeron et al., 2011). Their preferential consumption of tree shoots from species such as paper birch (*Betula papyrifera*), balsam poplar (*Populus balsamifera*), aspen, and mountain ash (*Sorbus* spp.) in winter determines which trees

will survive to grow in the spring (Speed et al., 2013). Only some of these trees will survive to the “escape height” where they will no longer be browsed. This has an effect on the overall composition of the forest as well as on nutrient cycling and litter composition. Unbrowsed species create a leaf litter that is slow to decompose and low in nutrients (Pastor and Danell, 2003). Their presence means that a forest inhabited by moose is quite different from one not inhabited by moose (Sinclair, 2003; Speed et al., 2013).

Due to their size and unique antlers, moose are a popular attraction for hunters and wildlife watchers in North America (Nadeu et al., 2017). Some states, such as Montana, auction off a few special hunting permits to the highest bidders each year, which allows the awardee to hunt moose anywhere in the state. The revenue from regular and special licenses goes to continued conservation efforts in Montana (DeCesare et al., 2014). The most recent report released by the United States Census and the United States Fish & Wildlife Service estimated that $26.2 billion and $75.9 billion were spent in 2016 by hunters and wildlife watchers, respectively. These figures include costs of trip-related food, lodging, and equipment as well as license fees

Between 2005 and 2015, the population of moose in Minnesota decreased by 60%. Montana’s moose population has also decreased (DeCesare et al., 2014). Declines are occurring in many places, though the Minnesota decline is particularly striking. One post-hunting season survey showed declines in Alberta, Saskatchewan, Manitoba, and Newfoundland, and in the states of Idaho, Wyoming, Montana, Minnesota, Vermont, and New Hampshire between the end of the 2014 season and the end of the 2015 season (Timmerman and Rodgers, 2017).

Declines are present even though population ratios of calf:cow and bull:cow remain stable. These ratios indicate the decline is not due to poor recruitment. Rather, adult mortality appears to be leading to decline, which is possibly caused by a disease event (Jones et al., 2017). Recent research on necropsy findings in moose suggest that there has been an increase in parasite infections in recent years.

Parasitic Infections of Moose

Winter ticks (*Dermacentor albipictus*) are a substantial threat to moose in North America. These winter ticks are a single-host species: all three life stages occur on the same individual host. When moose try to remove the engorged ticks, they often remove portions of their protective hair coat. The ticks make them anemic, and they cannot stay warm enough without their coat. This often results in death due to blood loss and increased energy expenditure when food is scarce. In addition, there is a correlation between winter tick infection and low fecundity in moose (Jones et al., 2017). The adults die and there are not enough young to replace them, which results in population declines.

Giant liver flukes (*Fascioloides magna*) have been found during necropsies of moose in the Great Lakes region, where this parasite is enzootic. Moose serve as an aberrant host for *F. magna*. When a moose ingests the infective cercariae or metacercariae, the parasite enters the gut, penetrates the intestinal wall, and migrates to the liver (Malcicka, 2015). Wünschmann et al. (2015) found hepatic lesions consistent with *F. magna* in 60% of moose necropsied in Minnesota between 2003 and 2013, but concluded that this parasite was unlikely to be the cause of death.

The meningeal worm (*Parelaphostrongylus tenuis)* is a common parasite of white-tailed deer in the eastern United States. Due to climate change and its effect on winters in North America, white-tailed deer have moved into moose habitats where they previously were not present. Shorter, milder winters have also enabled terrestrial gastropod hosts to proliferate in the same areas. As a result, the conditions are optimal for *P. tenuis* transmission (Lankester, 2010; Lankester, 2018). Since moose are an aberrant host for this parasite, the ingested infective larvae migrate through the spinal cord, causing damage to the central nervous system (Nagy, 2004). This may present as lameness, hindquarter weakness, and recumbency (Hartnack, 2017). Associations between moose declines, high density of white-tailed deer, and *P. tenuis* infections in some areas have been documented (Lankester, 2010).

Recent research indicated that the nematode *Elaeophora schneideri* is present in the moose population and tabanid flies in Minnesota (Grunenwald et al. 2018). These

nematodes are commonly referred to as “arterial worms,” as they reside within the major arteries in the definitive hosts (Hibler and Adcock, 1935). It is possible that the emergence of *E. schneideri* is a factor in the recent, sharp population decline in the Minnesota moose population, and it may be a factor in other declines as well. Research has yet to isolate a definitive causal factor of population declines.

Introduction to *Elaeophora schneideri*

Elaeophora schneideri is a filarial nematode of the family Onchocercidae. It was initially described in 1935 in domestic sheep (Wehr and Dikmans, 1935; Hibler and Adcock, 1968). Like other nematodes, they have a non-cellular cuticle which is secreted by the epidermis and overlaid with a glycoprotein surface coat. They are dioecious and sexually dimorphic; adult females measure up to 120 millimeters long and 810 micrometers wide, and males measure up to 65 millimeters long and 730 micrometers wide. Males have a coiled tail, which may be used for mating (Roberts et al., 2013).

After sexual reproduction, mature female *E. schneideri* produce live microfilariae (230-160 um x 10-13 um), which migrate from the arteries to the dermal capillaries of the host’s face and forehead (Worley et al., 1972). The microfilariae are taken up by a horsefly of the family Tabanidae when it takes a blood meal from a host. Once in the horsefly vector, the larvae invade the fat bodies lining the abdomen. They then move to the hemocoel where they develop for 2-3 weeks before migrating to the fly’s salivary glands as infective third-stage larvae (L3). The infective L3s are transmitted when the vector bites the skin of a new host (Hibler and Metzger, 1974).

Third-stage larvae remain in the new host’s dermis for 6-12 hours before migrating to the heart via venous circulation. Upon entering the lungs, they transition into arterial circulation, where they develop to adulthood. Mature nematodes primarily inhabit the cephalic and carotid arteries and their terminal branches, resulting in circulatory impairment of the cranial region (Hibler and Adcock, 1968). This can lead to ischemic necrosis of the brain, eyes, optic nerves, ears, muzzle, and other tissues of the head (Adcock and Hibler, 1969; Lankester, 2001). The resulting clinical signs characterize elaeophorosis, the disease caused by *E. schneideri*.

Elaeophora schneideri has previously been reported in the western and southwestern United States, though in more recent years the parasite has been reported in the southeast (Prestwood and Ridgeway, 1972; Lankester, 2001). The full extent of *E. schneideri*'s range is unknown.

Host-Parasite Interactions

Elaeophorosis has been reported in multiple domestic and wild ungulate species of the Cervidae and Bovidae families. Mule deer (*Odocoileus hemionus*) and black-tailed deer (*O. h. columbianus*) seem to be the most well-adapted hosts, as they rarely show clinical signs of *E. schneideri* infection. Thus, they are considered the normal definitive hosts (Hibler and Adcock, 1968). However, *E. schneideri* can undergo sexual reproduction in many ungulate species and therefore has several abnormal definitive hosts.

Though the pathogenesis is similar in all abnormal host species, the clinical signs of elaeophorosis vary. Mule deer and black-tailed deer generally do not present with clinical signs under natural or experimental conditions despite confirmed diagnosis on necropsy (Hibler et al., 1970; Pence and Gray, 1981; Couvillion, et al., 1986). White-tailed deer have been observed with oral impactions and impaired mylohyoideus muscles after experimental infection (Couvillion et al., 1986). Elk may present with blindness and gangrene due to ischemic necrosis of the optic nerves and tissues of the head, which is caused by microfilariae obstructing blood vessels (Adcock and Hibler, 1969). Barbary sheep (*Ammotragus lervia*), bighorn sheep (*Ovis canadensis*), and domestic sheep (*Ovis aries*) present with moderate-to-severe scabbed lesions on the head and face (Hibler et al., 1970; Pence and Gray, 1981), likely the result of thrombosis in dermal vessels and ischemic necrosis of the surrounding skin.

The first recognized case of elaeophorosis in a moose was in Montana in 1971 (Worley et al.,1972). Clinical signs and gross anatomic lesions in moose include ataxia, ear sloughing or cropping (Madden et al., 1991; Henningsen et al. 2012), fibrous arterial intimal proliferation (Levan et al., 2013; Worley et al., 1972), blindness, thrombosis, hemorrhage (Worley et al., 1972) and sudden death (Wehr and Dikmans, 1935; Hibler

and Metzger, 1974). In moose, disease severity can greatly vary among individuals. In some individuals, small burdens of *E. schneideri* can result in death; in others, larger burdens result in no clinical signs (Worley et al.,1972).

Previous research has suggested that moose have an inherent lack of resistance to elaeophorosis (Hibler and Metzger 1974; Worley 1975). However, some healthy moose examined in Colorado had carotid arterial proliferation consistent with *E. schneideri* infections, yet no worms were recovered from these individuals. This suggests that some moose may recover from infection (Henningsen et al. 2012; Levan et al., 2013).

Diagnosis of *Elaeophora schneideri*

Currently available methods for determining *Elaeophora schneideri* infection status are costly and labor-intensive, and often require observation of adult nematodes in the blood vessels of recently deceased moose on necropsy (Madden et al., 1991; Levan et al., 2013; Grunenwald et al., 2018; Wunschmann et al., 2015). Previously developed laboratory techniques (e.g. western blot) are time-consuming and non-quantifiable. Diagnosis based on symptoms alone is unreliable since there is a high level of variability in clinical presentation. The lack of a definitive diagnostic test has made the prevalence and clinical significance of this parasite difficult to assess.

Previous research revealed several proteins extracted from adult *E. schneideri* nematodes are reactive to seropositive moose serum and nonreactive to seronegative serum during a 2D western blot (Grunenwald, 2015). Fifteen of these peptide sequences were selected for purification and further testing using the Kolasker and Tongaonkar Antigenicity Scale (Kolaskar and Tongaonkar, 1990), Bepipred Linear Epitope Prediction (Larsen et al., 2006), and the Parker Hydrophobicity Scale (Parker et al., 1986) to assess the antigenic potential of the peptides. This study was unable to identify any peptides that bound only the *E. schneideri*-positive moose serum.

CHAPTER II

THE TRANSCRIPTOME OF *ELAEOPHORA SCHNEIDERI*

Background

The transcriptome is the entire set of functional genes that undergo transcription and ultimately lead to the production of gene products in a cell. The parasite transcriptome plays a role in host-parasite interactions, particularly where the immune system is concerned (Cancela et al., 2010; McTaggart et al., 2015). For example, antigens are most often peptides, which are encoded by mRNA contained within the transcriptome.

In order to acquire the transcriptome of a eukaryotic organism, introns must be removed, which is naturally accomplished by the mRNA splicing process. In the current published literature, there is only scant information on the genetics of *Elaeophora schneideri.* This problem persists for many parasites, as they have large genomes compared to other pathogenic organisms (e.g. bacteria) (Leroy et al., 2003).

Many diagnostic tools for parasites rely on knowledge of certain genes or proteins of the parasite of interest. It is difficult to ascertain this information without the transcriptome.

Nucleic Acid Extraction and Whole-Genome Sequencing

All nematode samples were previously collected by our collaborators from 2012-2015 and sent to the Molecular Parasitology Research Lab at UT College of Veterinary Medicine where they were stored at -80°C. I extracted DNA from a section of a thawed, whole *Elaeophora schneideri* nematode stored in phosphate-buffered saline (PBS, pH = 7.2) using the MasterPure DNA Purification Kit (EpiCenter Technologies, Chicago, Illinois) per manufacturer protocol for tissue samples and total nucleic acid preparation. Then, I prepared the DNA library using the Nextera XT DNA Library Preparation Kit (Illumina, San Diego, California) per manufacturer protocol.

Due to the tendency of RNA to rapidly degrade and the importance of its integrity for this experiment I selected a whole nematode that had been collected from the carotid artery of a female moose 30 hours postmortem, rinsed with PBS, and immediately stored in RNAlater (Invitrogen, Carlsbad, California) for RNA extraction. I performed the extraction using the Nucleospin RNA Kit (Macherey-Nagel, Germany).

The resulting extract had a concentration of 109.1 ng RNA per µL, which I confirmed using a NanoDrop Microvolume Spectrophotometer. I prepared the RNA library for sequencing using the SMART-Seq v4 Ultra Low Input RNA Kit for Sequencing (TakaraBio, Japan). The output of this kit was complementary DNA (cDNA), which is produced through reverse transcription and allows for stable cloning of the gene of interest in downstream applications.

We used MiSeq Technology (Illumina) to sequence the DNA and mRNA, then assembled the resulting reads with SeqMan NGen 14 software (DNASTAR, Madison, Wisconsin). The resulting output was a FASTA text file of sequence reads, each with a unique identifying number. We ran a simple shell script on the text file to translate the nucleic acid sequences into amino acid transcripts while keeping the IDs with their associated sequences. We made a separate file for each of the three forward and three reverse reading frames, resulting in a total of six files of amino acid transcripts.

IgG-Assisted Peptide Identification

In order to identify immunogenic proteins useful for serologic tests, we solubilized and analyzed proteins from an *Elaeophora schneideri* nematode. For protein solubilization, we used a whole nematode that had been frozen and stored in PBS after being harvested from a deceased moose in Montana. We dipped the thawed nematode in liquid nitrogen for 15 seconds, then finely chopped it with a razorblade and deposited it into a 2.0 mL microcentrifuge tube. We added 100 µL PBS (pH = 7.2) to wash away any remaining moose blood and environmental contaminants, then centrifuged the tube at 16,000 times the force of gravity (xg) to separate the tissue from the PBS. After carefully decanting the supernatant, we added Radioimmunoprecipitation assay (RIPA) buffer (0.394g anhydrous Tris-HCl, 0.8766g NaCl, 1.0mL 1.0% Nonidet P-40, 1.0g 1.0% sodium deoxycholate, 0.1g 0.1% sodium dodecyl sulfate, combined in 100 mL distilled water) to the tube at a ratio of 4 mL RIPA Buffer per gram of tissue in the tube to solubilize the proteins. We incubated the tube at 4°C for 30 minutes, then vortexed the solution until it was homogenous. We centrifuged the homogenized solution at 13,000 rotations per minute (rpm) for 10 minutes at 4°C to pellet insoluble debris, which

resulted in approximately 400 µL of protein supernatant. We removed this supernatant and transferred it to a new, sterile 2.0mL microcentrifuge tube.

To identify antigenic peptides, we isolated relevant proteins from the sample based on immunoaffinity with moose IgG. We received thirteen positive control serum samples from collaborators in Alaska, Wyoming, and Montana. They collected the sera from moose with *Elaeophora schneideri* infection confirmed on necropsy. We stored the samples at -20°C. After removing 100 µL from ten of the positive control samples to create a 1 mL pooled serum sample, we isolated IgG from the serum using protein A/G affinity chromatography with the Nab Protein Spin Kit for Antibody Purification (Thermo Scientific, Waltham, Massachusetts) per manufacturer protocol. This produced three fractions of IgG solution with the following concentrations: 4.1487 mg/mL, 3.9851 mg/mL, and 0.9061 mg/mL.

We biotinylated the most concentrated fraction using EZ-Link Sulfo-NHS-LC-Biotin (Thermo Scientific, Waltham, Massachusetts) per manufacturer protocol for biotinylating proteins in solution. Since biotin binds with high affinity to avidin, we would be able to adhere the IgG molecules to a monomeric avidin column, where they could capture antigens of interest. We used an indirect ELISA with chicken anti-cervid IgG to confirm biotinylation. We divided a Costar 3590 96-well flat-bottomed assay plate into four 12 x 2 well sections: the first was coated with PBS instead of biotinylated IgG and probed with PBS instead of anti-cervid IgG; the second was coated with PBS and probed with anti-cervid IgG; the third was coated with biotinylated IgG and probed with PBS; and the fourth was coated with biotinylated IgG and probed with anti-cervid IgG. If our Biotinylation procedure was successful, the final section of the plate would have significantly more optical density than the other three sections. This was the case, so we proceeded.

We combined the protein supernatant with 250µL of the previously prepared biotinylated antibody solution and incubated them at 37°C for one hour to bind the IgG to the solubilized *Elaeophora schneideri* proteins. We then passed the IgG-protein solution through a monomeric avidin column (ThermoFisher, Waltham, Massachusetts) per manufacturer protocol to separate the biotinylated, bound antibody-protein

complexes from the unbound proteins. After washing away the unbound proteins we eluted six 2 mL fractions from the column with protein concentrations of 0.3446 mg/mL, 0.3230 mg/mL, 0.1274 mg/mL, 0.2099 mg/mL, 0.2310 mg/mL, and 0.1995 mg/mL.

We submitted the most concentrated fraction (0.3446 mg/mL) to the Proteomics and Mass Spectrometry (PAMS) Core facility at the University of Georgia for sequence-guided LC-MS/MS analysis. They were able to distinguish the peptides from the antibodies, *in silico,* which they then compared to the six possible reading frames and predicted amino acid sequences of the transcriptome. Once we had these results, we searched for the source protein for each peptide using a text search of the transcript files. The fragments were only located in one of the six reading frames, so we were able to conclude this was the correct reading frame. The peptide fragments we received from PAMS belonged to four protein transcripts within this reading frame.

CHAPTER III
TESTS OF ANTIGENICITY OF *ELAEOPHORA SCHNEIDERI* PROTEINS

Synthetic Peptide Assay

To identify peptide antigens unique to *Elaeophora* schneideri, we (Dr. Stephen Kania, and I) analyzed the predicted amino acid sequence of each transcript of interest (see Chapter II) using the Basic Local Alignment Search Tool for proteins (BLASTp) (National Institutes of Health, National Center for Biotechnology Information (NCBI), Bethesda, Maryland) with default parameters. This allowed us to determine the degree of similarity of our sequences to sequences contained within the NCBI database. Similarity was based on BLAST's default Maximum Score and Query Cover scores.

We entered selected unique sequences into an online B-cell epitope prediction tool (IEDB Analysis Resource). We selected all predicted linear epitopes, between 10 and 30 amino acids in length, and examined them for similarity to cervid host species and related parasite species using BLASTp with parameters adjusted for short input.

Unique peptides were synthesized commercially (GenScript, >75% purity). I dissolved synthetic peptides in nuclease-free water to a final concentration of 1 milligram per milliliter. I used each of the synthetic peptides separately as antigens in trial enzyme-linked immunosorbent assays (ELISAs).

I selected one purified peptide for each plate. The final concentration of solubilized peptide was 1 µg/mL in PBS (pH 7.2). We added 100 µL of this solution to each well of a Corning® 96 Well EIA/RIA Assay Microplate (Millipore Sigma, Darmstadt, Germany). The plate was covered with aluminum foil prior to incubating it for one hour at 37°C. After the incubation, a BioTek ELX405R Microplate Washer was used to wash the plate three times with 200 µL 0.05% PBS-Tween (PBS-T). To prepare a blocking solution, I dissolved 0.5 g powdered skim milk in 10 mL PBS-T to create a 5% protein solution. I then added 100 µL of this blocking solution to each well of the assay plate, covered it with foil, and incubated it at 37°C for 10 minutes. The plate washer was used to aspirate the solution.

Sera (n = 9) from five-week-old white-tailed deer (*Odocoileus virginianus*) fawns, generally supplied by Dr. Michael Yabsley (University of Gerogia, Athens, Georgia) were used as negative control samples; currently *E. schneideri* is not known to be endemic to this area, and their young age made it unlikely that they were exposed to the

horsefly vector. As previously mentioned, our positive control samples (n=13) were collected by our collaborators from known *E. schneideri*-positive moose. I diluted 1 µL of each serum sample separately in microcentrifuge tubes containing 2.0 mL PBS-T. I added either 100 µL of diluted sample – which acted as the primary antibody – or 100µL PBS-T to assigned sections on the plate (Figure 1). The PBS blank in this step was used to isolate the binding effect of the moose serum antibodies from nonspecific background binding. I covered the plate and incubated it for 1 hour at 37°C. This incubation was followed with another set of three washes.

We structured the ELISA plate so that one-half of the 96-well plate would be used for 7 negative controls, and the other half for 7 positive controls. Each positive and negative control sample was assigned a unique number. We then used a random number generator to select samples for each plate until the 7 negative slots and the 7 positive slots were filled. Each sample was assigned a 3 x 2 section of wells on the plate (Figure 1). We always completed every procedure on the negative control sections of the plate prior to performing them on the positive control sections in order to prevent contamination. The secondary antibody, chicken anti-cervid IgG conjugated with horseradish peroxidase (HRP) (Exalpha Biologicals, Inc., Shirley, Massachusetts), was diluted in PBS-T to achieve a final concentration of 0.05% antibody. I added 100 µL of this diluted secondary antibody solution to each well of the assay plate. I incubated this at 37°C for one hour to allow the anti-cervid antibody to bind to the moose antibodies. I then added 100 µL 3,3',5,5'-tetramethybenzidine (TMB) substrate (Thermo Scientific, Waltham, Massachusetts) to each well, covered the plate, and allowed it to incubate, at room temperature, in the dark for 15-30 minutes. After sufficient color developed, I added the stop solution (0.16M sulfuric acid) to stop the reaction and change the color from blue to yellow. I then read the optical density values using a BioTek ELx800

	1	2	3	4	5	6	7	8	9	10	11	12
A	PBS	PBS	PBS	Neg4	Neg4	Neg4	PBS	PBS	PBS	Pos4	Pos4	Pos4
B	PBS	PBS	PBS	Neg4	Neg4	Neg4	PBS	PBS	PBS	Pos4	Pos4	Pos4
C	Neg1	Neg1	Neg1	Neg5	Neg5	Neg5	Pos1	Pos1	Pos1	Pos5	Pos5	Pos5
D	Neg1	Neg1	Neg1	Neg5	Neg5	Neg5	Pos1	Pos1	Pos1	Pos5	Pos5	Pos5
E	Neg2	Neg2	Neg2	Neg6	Neg6	Neg6	Pos2	Pos2	Pos2	Pos6	Pos6	Pos6
F	Neg2	Neg2	Neg2	Neg6	Neg6	Neg6	Pos2	Pos2	Pos2	Pos6	Pos6	Pos6
G	Neg3	Neg3	Neg3	Neg7	Neg7	Neg7	Pos3	Pos3	Pos3	Pos7	Pos7	Pos7
H	Neg3	Neg3	Neg3	Neg7	Neg7	Neg7	Pos3	Pos3	Pos3	Pos7	Pos7	Pos7

Figure 1. An example of the layout for an ELISA plate. Each half (left or right) of the plate has one 3x2 set of wells for the PBS blank control and seven 3x2 sets of wells for the negative or positive control serum samples, which we added after incubating the plate with antigen, washing the plate, blocking the plate with 0.05% skim milk, and aspirating the blocking solution. Shading on alternating blocks is to assist with visibility.

I calculated the relative optical density (ROD) values by subtracting the mean value of the PBS blank wells from the raw optical density score for each well (Figure 2). The six RODs for each sample were then averaged to obtain a mean ROD for each sample. The 7 mean RODs for each population were then averaged to obtain a negative control population mean and a positive control population mean. I then ran a T-test to determine whether the population means were significantly different ($p < 0.05$).

Recombinant Protein Production and Purification

Through our original analysis of the transcriptome data, we identified four amino acid sequences with sections unique to *Elaeophora schneideri*. However, we found the final five peptides we used in our synthetic peptide assay were found in two of the four amino acid sequences. We therefore decided to proceed with these two sequences as “source protein transcripts” for our protein antigens. Since each amino acid contig was

	A	B	C	D	E	F	G	H	I	J	K	L
1	0.1	0.087	0.058	1.787	1.823	1.925	0.063	0.066	0.067	1.735	1.728	1.885
2	0.056	0.064	0.064	1.641	1.682	1.737	0.049	0.049	0.049	1.678	1.72	1.782
3	0.286	0.247	0.25	0.772	0.805	0.831	0.328	0.312	0.3	0.299	0.296	0.365
4	0.294	0.248	0.26	0.773	0.818	0.853	0.353	0.348	0.316	0.272	0.301	0.411
5	2.718	2.537	2.504	0.851	0.945	1.015	0.471	0.451	0.437	0.902	0.878	0.909
6	2.636	2.434	2.484	0.859	0.896	0.948	0.487	0.415	0.403	0.831	0.896	0.984
7	1.148	0.975	0.994	0.988	1.019	0.977	0.51	0.427	0.444	1.495	1.489	1.676
8	1.191	1.062	1.072	1.209	1.216	1.103	0.686	0.694	0.542	1.644	1.699	2.093
9												

Figure 2. An example of a 96-well ELISA plate readout showing optical density (OD) after export into Excel. Each cell represents a single well on the plate. Each blank or sample was given a 2x3 well section. The PBS blank sections -- which were coated only with PBS and not the antigen -- are outlined in black rectangles. The black line between columns F and G represents the demarcation between wells treated with negative control serum (on the left) and wells treated with positive control serum (on the right). Relative optical density (ROD) readings were obtained by subtracting the average value of the PBS blank wells from the raw OD scores. For this plate, the average OD for the PBS blank wells is 0.064. Therefore, the ROD for each well would be OD - 0.064. After obtaining RODs, the six values for each sample would be averaged to obtain a mean ROD for each sample.

given a unique identifying number corresponding to the number on its encoding nucleotide contig, we were able to locate the original mRNA transcript for each protein. We entered the nucleotide sequences into ORFfinder (NCBI), which resulted in a single open reading frame of amino acids for each protein transcript. These open reading frame amino acid sequences will be further referred to by their identifying numbers: cl107190 (282bp) and cl47386 (890 bp) or collectively as “insert sequences” in this document.

The insert sequences were codon optimized for expression in *E. coli,* synthesized, and inserted into pET100/D-TOPO plasmids by GeneArt (Invitrogen, Carlsbad, California) (Figure 3). Aside from the insert sequences (cl47386 and cl107190), the two gene constructs were identical. The constructs included a sequence encoding six consecutive histidine residues, which results in the production of a polyhistidine “tag” or 6xHis-tag on the expressed protein. The 6xHis-tag enables detection of the protein in downstream applications by using an antibody or substrate that binds directly to the chain of histidine residues.

I inserted these constructs into chemically competent DH10B *Escheria coli* cells using Novagen’s standard heat shock transformation protocol. I plated the transformed cells on Luria-Burtani agarose plates containing 50 µg/mL ampicillin and cultured them

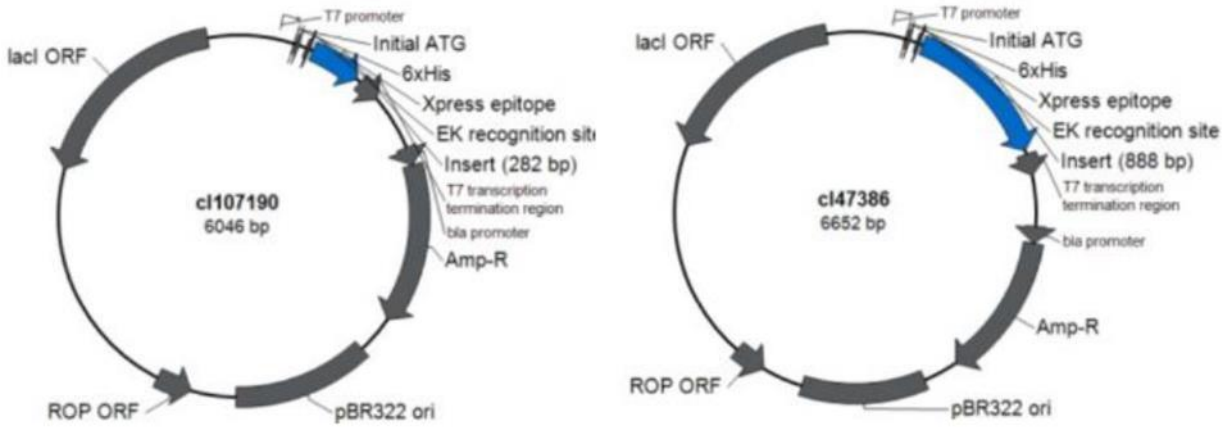

Figure 3. Comparison of the *E. coli*-optimized plasmids with inserts for cl`07`90 and cl47386. The constructs are identical except for the inserts. The construct also contains a gene for ampicillin resistance and a transcript for the 6xHis-tag (6xHis on the picture).

overnight at 37°C. If the cultures grew successfully, I stored the plates at 4°C for up to four weeks.

To induce protein expression, I removed one isolated colony of transformed cells from the agarose plate using a sterile plastic loop and deposited it into 5 mL of Luria-Burtani (LB), Miller broth (Fisher Bioreagents, Pittsburg, Pennsylvania) with 0.1 mg/mL ampicillin. This tube was incubated for 3 - 6 hours at 37°C on a 250 rpm shaker. After incubation, I removed 20 µL of the 5 mL liquid culture and deposited it into an Erlenmeyer flask containing 100 mL room-temperature LB (Miller) broth with 0.1 mg/mL ampicillin. This flask was incubated for 3 hours on a 250 rpm shaker at 37°C. After this incubation, I checked the turbidity of the culture by depositing 2 mL of cultured broth into a clear tube and comparing it to a clear reference tube of uncultured LB broth. We held both tubes up to a piece of white paper with black text printed on it; if there was a slight increase in turbidity which was visible to the eye, the black text would be blurred and slightly distorted compared to the black text when viewed through the uncultured broth. If the turbidity had increased, we would induce protein expression with 1M Isopropyl β-D-1-thiogalactopyranoside (IPTG); the final concentration of IPTG in the flask was 0.5 mM. This was incubated overnight (≤ 18 hours) at 37°C on a 250 rpm shaker in order to allow maximum cell growth and protein expression.

The following morning, I distributed the cultured broth equally into six 15 mL Nunc™ conical flasks (Thermo Scientific, Waltham, Massachusetts), then centrifuged them at 4000 xg at 4°C for 15 minutes. I then carefully decanted the supernatant and discarded it. I resuspended the bacterial pellet in each tube in 1 mL PBS (pH = 7.2) by pipetting the suspension up and down with a 1000 µL pipette, then consolidated the bacteria suspensions into a single 15 mL conical tube. Centrifugation at 4000 xg at 4°C for 15 minutes was then repeated and the supernatant discarded. The cell pellet was then frozen overnight at -20°C to assist with cell lysis.

BugBuster Protein Extraction Reagent (Novagen, Madison, Wisconsin) with Halt® 100X Protease Inhibitor Cocktail (Thermo Scientific, Waltham, Massachusetts) was used to lyse the cells per manufacturer protocol for soluble fraction and inclusion body purification. I evaluated the protein content of these extracts using a single-step Bradford protein assay (Bio-Rad, Hercules, California) using bovine serum albumin dilutions as comparative protein standards.

Proteins were separated using SDS-PAGE on a precast NuPAGE 10% bis-tris 2D polyacrylamide gel (Invitrogen, Carlsbad, California). After electrophoresis, I electrophoretically transferred the resolved proteins to a 0.2 µm nitrocellulose membrane (Thermo Scientific, Waltham, Massachusetts) (Towbin et al., 1979; Mahmood and Yang, 2012). I placed the western blot in 5% skim milk PBS-T blocking solution and placed it on an orbital shaker at low speed for one hour at room temperature (approximately 22°C) to reduce nonspecific binding in future steps. The blocking solution was then discarded.,I cut the membrane into 3 mm strips, and put the strips into an 8-channel plastic tray with a lid. To probe the blot with Anti-6XHis-tag antibody (ABCam) I diluted the antibody 1:100 in PBS-T, inverted the tube to mix, and deposited 100 µL aliquots of the solution onto the membrane strips. I placed the tray on an orbital shaking platform for one hour at low speed at room temperature to evenly distribute the probing antibody on the strips.

After this incubation, I washed the membrane strips by covering each strip with 500 µL PBS-T and placing the tray on the orbital shaking platform at room temperature for ten minutes, then discarded the wash solution. This was repeated two more times for

a total of three washes. I then added 4-chloro-1-napthol (4C1N) substrate, which reacts with the horseradish peroxidase on the probing antibody. This allows visualization of the protein bands that were bound by that antibody.

To probe the western blots with moose sera, I diluted each serum sample 1:100 in PBS-T and added 100 µL of diluted serum to each strip. We placed the tray on the orbital shaker for one hour at room temperature, then proceeded with three washes. We HRP-conjugated chicken anti-cervid IgG (Gallus Immunotech, Atlanta, Georgia) was used as the secondary antibody. I diluted this antibody 1:500 in PBS-T and deposited 100 µL aliquots onto each strip in the tray. I placed the tray on the orbital shaker for one hour at room temperature, then added 4C1N. This was incubated without shaking, in the dark, at room temperature. I then compared the developed bands to a standard protein ladder to estimate the size of the reactive proteins.

CHAPTER IV
RESULTS AND DISCUSSION

Synthetic Peptide Assay

We selected the five peptides with the lowest BLASTp similarity scores for use as templates for synthetic peptides (Table 1). We evaluated similarity to other sequences in the BLASTp database using the E-value – the number of alignments expected by chance with a particular score or better – and Max Score. A low E-value corresponds to low similarity between the searched sequence and the most similar result. Maximum score is a value that depends on the number of certain types of alignments and mismatches, and has the same conceptual framework as E-value. The scores and E-values were low for every peptide, which indicates the sequences are unique. Many of the closest matches to each of the five peptides were from other known nematode proteins. Predicted peptides and proteins were not considered.

The plate reader outputs for the ELISAs were evaluated using Microsoft Excel and an online comparison of means calculator (MedCalc). The ROD for each serum sample was consistent within each trial; however, there was considerable variation for each serum sample between trials (Figure 4).

None of the peptides showed consistent results, and there were no significant differences between the positive and negative control means in any of the trials. We attempted to correct for this using chicken egg albumin and skim milk blocks, but this was not successful. Further, upon troubleshooting, we discovered there was no significant differences between plates coated with antigen and uncoated plates. This indicates that the antibodies in the serum sample were binding directly to the assay plate, rather than to a plate-bound antigen. We confirmed this conclusion with a series of dot blots on nitrocellulose membranes, which enabled us to rule out problems with other binding interactions in the process.

Recombinant Peptides

Inserting the constructed plasmids into DH10B cells resulted in successful transformants that could be maintained on LB agarose plates with 50 µg/mL ampicillin.

Table 1. The physical characteristics and top BLAST result for the five synthetic peptides. Similarity to other sequence entries in the BLAST database was evaluated based on the E-value: the number of alignments expected by chance with a particular score or better. A low E-value corresponds to low similarity between the searched sequence and the most similar result. Maximum score is a value that depends on the number of certain types of alignments and mismatches, and has the same conceptual framework as E-value. The scores for the top match for each peptide in every category are low, which indicates the sequences are somewhat unique. Many of the closes matches to each of tehse peptides were known peptides from other nematodes. Predicted peptides and proteins were eliminated form consideration.

Sequence	Molecular weight (g/mol)	Isoelectric Point	Closest BLASTp Match	E-value	Maximum Score
VSTQSTGIQESQRNCPKMSTRTTAGG	2425.2	9.82	FAD-dependent oxidoreductase (*Ruegeria marina*)	20	33.3
SQRNCPKMSTRTTAGG	1694.9	11.48	Calponin protein 4 (*Wuchereria bancrofti*)	53	30.3
HTESHEVTTPQGQTSDSAEAH	2249.23	4.57	OmdA domain containing protein (*Streptomyces europaeiscabei*)	0.17	38.4
VQQQTPQQQQQQQKKGPTVPAKPGQTPITR	3354.75	11.93	Bm6544 (*Brugia malayi*)	2e-07	57.1
TESHEVTTPQGQTSDSAEAH	2112.09	4.14	OmdA domain containing protein (*Streptomyces europaeiscabei*)	0.17	38.4

Anti-His antibodies were used as primary antibodies to detect expressed proteins on the western blot strips. In most cases, no proteins appeared; we believe the his-tag may be attached to the N-terminus for our proteins, but the anti-His antibody is designed to bind to C-terminus his-tags. We tested the other binding steps in this process to ensure all other processes were working correctly, and they were.

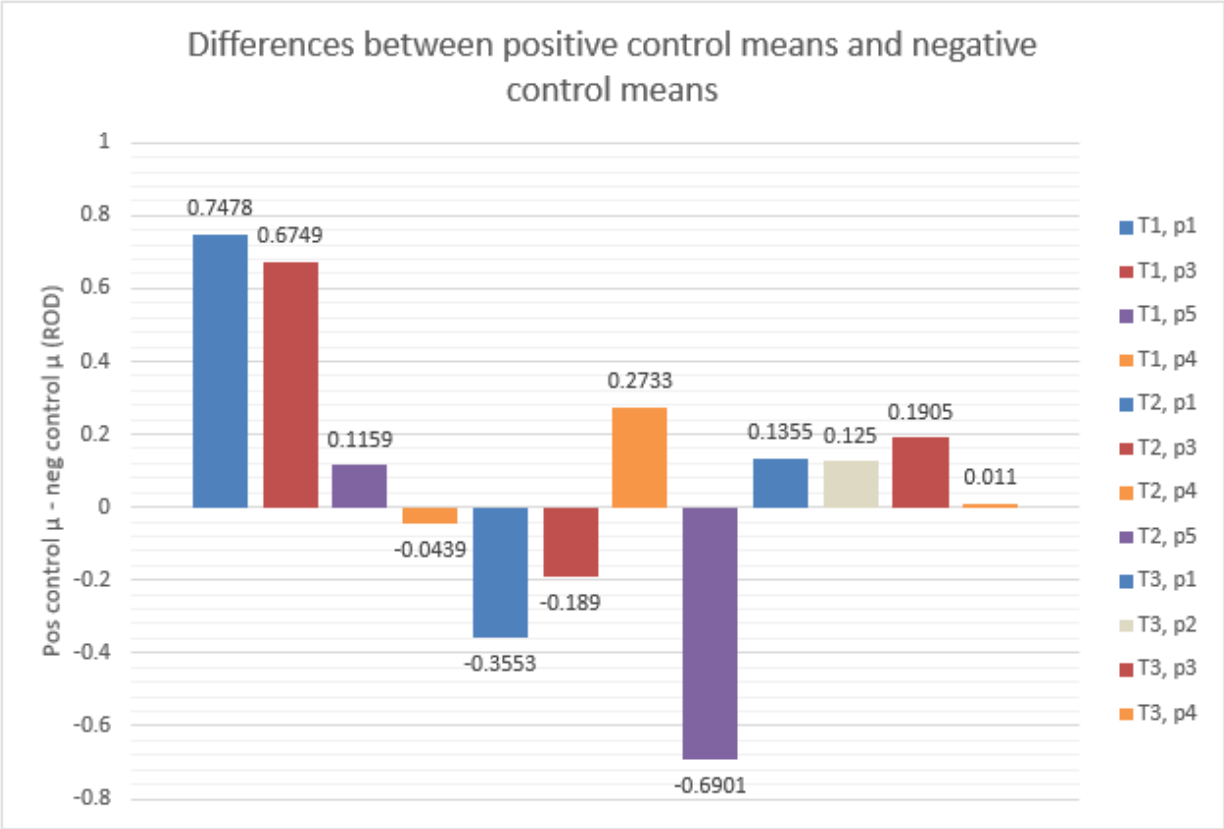

Figure 4. Differences in relative optical density values between the positive and negative control population means in the first three trials (T) of peptide (p) testing. Each bar represents one plate, which is coated with one of the five peptides as the antigen. Each peptide is represented by a single color, and each peptide was tested on no more than one plate per trial. A longer bar indicates a greater difference between the positive control population mean and the negative control population mean. Bars with negative values indicate that the negative control population mean was higher than the positive control population mean, which results in a negative overall value.

However, in one trial, discrete bands did appear (Figure 5). This blot was split into 11 strips: 4 were probed with anti-his antibody, 4 were probed with positive control sera, and 3 were probed with negative control sera. Dark bands appeared on the anti-His tag strips that corresponded with bands on the positive strips; there was no band in this area on the negative strips. This result was unable to be replicated. We believe this single result indicates that it is possible to express his-tagged proteins that also bind with *Elaeophora schneideri*-positive sera using synthetic gene constructs. However, the recombination and expression procedures must be optimized for the proteins we are trying to express.

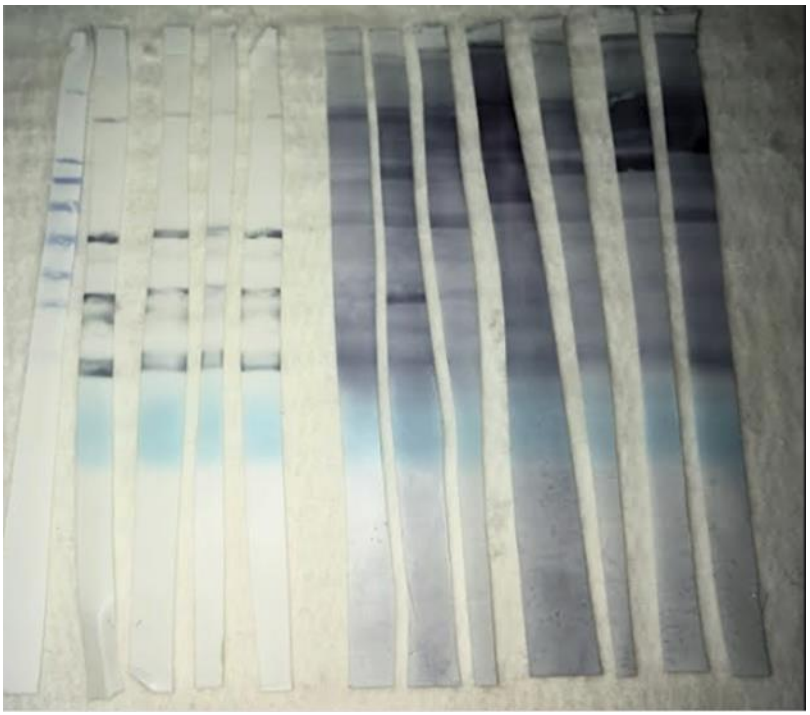

Figure 5. Strips of a western blot used to evaluate protein expression by cl107190 cells. These cells were lysed with N2 and underwent SDS PAGE on a 10% Tris-bis 2D gel, then transferred to a nitrocellulose membrane. The leftmost strip is the standard (or ladder) and the bands correspond to proteins of different weights. From top to bottom: 198 kilodaltons (kDa), 62 kDa, 49 kDa, 38 kDa, 28 kDa, 18 kDa, 14 kDa, 6 kDa, and 3 kDa. The next four strips to the right were probed with 6x Anti-His HRP antibody. The following four strips were probed with positive control serum, and the last three strips with negative control serum. There is a dark protein band that appears on the strips probed with 6x Anti0His antibody at approximately the 10 kDa spot. There is a dark band that appears in the same spot on one of the positive control strips, and a faint band in the same spot on another positive control strip. This band does not appear on any of the negative control strips. This suggests that the positive serum is binding to the 107190 protein, which has a weight of 8.94 kDa.

CONCLUSION

To date this is the first description of the transcriptome of *Elaeophora schneideri* and the first attempt to identify its antigenic proteins.

Due to the conserved nature of the nematode genome, the transcriptome reported herein may provide the foundation for further research on other parasitic nematodes, including those that commonly parasitize humans. In addition, this information will further allow scientists to isolate unique antigens for nematodes such as *Haemonchus contortus* and *Ostertagia ostertagi*, which parasitize food animals.

Recombination and expression of the antigenic proteins must be optimized before a serological diagnostic assay for *Elaeophora schneideri* can be fully realized. Analyzing the chemical and physical structure of the proteins in order to get a sense of the ideal parameters may assist in this process.

Once the purified antigens are available for the assay, it should be straightforward to optimize and develop a diagnostic ELISA. Due to the volume and variety of moose sera contained in UTCVM's freezer archive, this diagnostic ELISA will enable generation of vital baseline data for future study of *Elaeophora schneideri*. Since it is likely that climate change has been affecting the transmission of this parasite, this data may provide a model that other ecologists can study to predict further spread of other nematodes that utilize cervids as hosts, such as *Parelaphostrongylus tenuis* and *Rumenfilaria andersoni*.

REFERENCES

Adcock JL, Hibler CP. 1969. Vascular and Neuro-ophthalmic Pathology of Elaeophorosis in Elk. *Veterinary Pathology* 6: 185-213.

Belovsky G, Jordan P. 1981. Sodium Dynamics and Adaptations of a Moose Population. *Journal of Mammology* 62(3):613-621.

Bergeron DH, Pekins PJ, Jones HF, Leak WB. 2011. Moose Browsing and Forest Regeneration: A Case Study in Northern New Hampshire. *Alces* 47: 39-51.

Bubenik GA, Bubenik PG. 2008. Palmated Antlers of Moose May Serve as a Parabolic Reflector of Sounds. *European Journal of Wildlife Research* 54: 533-535.

Cancela M, Ruetalo N, Dell'Oca N, da Silva E, Smircich P, Rinaldi G, Roche L, Carmona C, Alvarez-Valin F, Zaha A, Tort JF. 2010. Survey of Transcripts Expressed by the Invasive Juvenile Stage of the Liver Fluke *Fasciola hepatica*. *BMC Genomics* 11: 227.

Cederlund G, Sand J. 1994. Home-Range Size in Relation to Age and Sex in Moose. *Journal of Mammology* 75(4): 1005-1012.

Clinton DW. 1822. Letter XLIV. In: *Letters on the Natural History and Internal Resources of the State of New York*, Hibernicus. Bliss and White, New York, New York, 189-193.

Clutton-Brock TH. 1982. The Functions of Antlers. *Behaviour* 79(2): 108-124.

Clutton-Brock TH, Albon SD. 1980. Antlers, Body Size, and Breeding Group Size in the Cervidae. *Nature* 285: 565-567.

Couvillion E, Nettles VF, Rawlings CA, Joynep RL. 1986. Elaeophorosis in White-Tailed Deer: Pathology of the Natural Disease and Its Relation to Oral Food Impactions. *Journal of Wildlife Diseases* 22: 214-223.

Dannel K, Edenius L, Lundberg P. 1991. Herbivory and Tree Stand Composition: Moose Patch Use in Winter. *Ecology* 72(4) 1350-1357.

DeCesare N, Smucker T, Garrot R, Gude J. 2014. Moose Status and Management in Montana. *Alces* 50: 35-51.

Grunenwald CM, Butler E, Wunschmann A, Armien A, Carstensen M, Hildebrand E, Moon RD, Gerhold RW. 2018. Emergence of the Arterial Worm *Elaeophora schneideri* in Moose (*Alces alces*) and Tabanid Fly Vectors in Northeastern Minnesota, USA. *Parasites and Vectors* 11: 1-11.

Grunenwald CM. 2015. *Epidemiology of Select Species of Filarial Nematodes in Free-Ranging Moose (Alces alces) of North America.* Ph.D. Thesis, Comparative and Experimental Medicine, University of Tennessee, Knoxville, Tennessee, USA, 76 pp.

Hartnack AK. 2017. Spinal Cord and Peripheral Nerve Abnormalities of the Ruminant. *Veterinary Clinics of North America - Food Animal Practice* 33: 101-110.

Henningsen C, Williams A, Tate M, Kilpatrick S, Walter WD. 2012. Distribution and Prevalence of *Elaeophora schneideri* in Wyoming. *Alces* 48: 35-44.

Hibler CP, Metzger CJ. 1974. Morphology of the Larval Stages of *Elaeophora schneideri* in the Intermediate and Definitive Hosts with Some Observations on their Pathogenesis in Abnormal Definitive Hosts. *Journal of Wildlife Diseases* 10: 361-369.

Hibler CP, Adcock JL. 1968. Redecription of *Elaeophora schneideri* Wehr and Dikmans, 1935 (Nematoda: Filaroidea). *Journal of Parasitology* 54: 1095-1098.

Hibler CP, Adock JL, Gates GH, White R. 1970. Experimental Infection of Domestic Sheep and Mule Deer with *Elaeophora schneideri* Wehr and Dikmans, 1935. *Journal of Wildlife Diseases* 6(2): 110-111.

Jones H, Pekins P, Kantar LE, O'Neil, Ellingwood D. 2017. Fecundity and Summer Calf Survival of Moose During 3 Successive Years of Winter Tick Epizootics. *Alces* 53: 85-98.

Kie JG. 1999. Optimal Foraging and Risk of Predation: Effects on Behavior and Social Structure in Ungulates. *Journal of Mammology* 80: 1114-1129.

Kolaskar AS, Tongaonkar PC. 1990. A Semi-Empirical Method for Prediction of Antigenic Determinants on Protein Antigens. *FEBS Letters* 276: 172-174.
Lankester MW. 2001. Extrapulmonary Lungworms of Cervids. In: *Parasitic Diseases of Wild Mammals*, 2nd Ed., editors Samuel WM, Pybus MJ, Kocan AA. Iowa State University Press, Ames, Iowa, 228-278.
Lankester MW. 2010. Understanding the Impact of Meningeal Worm, *Parelaphostrongylus tenuis*, on Moose Populations. *Alces* 46: 53-70.
Lankester MW. 2018. Considering Weather-Related Transmission of Meningeal Worm, *Parelaphostrongylus tenuis*, and Moose Declines. *Alces* 54: 1-13.
Larsen JE, Lund O, Nielson M. 2006. Improved Method for Predicting Linear B-Cell Epitopes. *Immunome Research* 2.
Leroy S, Duperray C, Morand S. 2003. Flow Cytometry for Parasite Nematode Genome Size Measurement. *Molecular and Biochemical Parasitology* 128: 91-93.
Levan IK, Fox KA, Miller MW. 2013. High Elaeophorosis Prevalence Among Harvested Colorado Moose. *Journal of Wildlife Diseases* 49: 666-669.
Madden DJ, Spraker TR, Adrian WJ. 1991. *Elaeophora schneideri* in moose (*Alces alces*) from Colorado. *Journal of Wildlife Diseases* 27: 340-341.
Mahmood T, Yang P. 2012. Western Blot: Technique, Theory, and Trouble Shooting. *North American Journal of Medical Sciences* 4(9): 429-434.
Malcicka M. 2015. Life History and Biology of *Fascioloides magna* (Trematoda) and its Native and Exotic Hosts. *Ecology and Evolution* 1381-1397.
Matthews PE. 2012. History and Status of Moose in Oregon. *Alces* 48: 63-66.
McTaggart SJ, Cezard T, Garbutt JS, Wilson PJ, Little TJ. 2015. Transcriptome Profiling During a Natural Host-Parasite Interaction. *BMC Genomics* 16: 643.
Miller GS. 1899. A New Moose from Alaska. *Proceedings of the Biological Society of Washington* 13: 57-59.
Miquelle DG. 1983. Browse Regrowth and Consumption Following Summer Defoliation by Moose. *The Journal of Wildlife Management* 47(1): 17-24.
Nadeu SM, DeCesare NJ, Brimeyer DG, Bergman EJ, Harris RB, Hersey KR, Huebner KK, Matthews PE, Thomas TP. 2017. Status and Trends of Moose Populations and Hunting Opportunity in the Western United States. *Alces* 53: 99-112.
Nagy DW. 2004. *Parelaphostrongylus tenuis* and Other Parasitic Diseases of the Ruminant Nervous System. *Veterinary Clinics of North America - Food Animal Practice* 20: 393-412.
Nelson EW. 1914. Description of a New Subspecies of Moose from Wyoming. *Proceedings of the Biological Society of Washington* 27: 71-73.
Parker JM, Guo D, Hodges RS. 1986. New Hydrophilicity Scale Derived from High-Performance Liquid Chromatography Peptide Retention Data: Correlation of Predicted Surface Residues with Antigenicity and X-Ray-Derived Accessible Sites. *Biochemistry* 25: 5425-5432.
Pastor J, Dannell K. 2003. Moose-Vegetation-Soil Interactions: A Dynamic System. *Alces* 39: 177-192.
Peek JM, LeResche RE, Stevens DR. 1974. Dynamics of Moose Aggregations in Alaska, Minnesota, and Montana. *Journal of Mammology* 55(1): 126-137.
Pence B, Gray G. 1981. Elaeophorosis in Barbary Sheep and Mule Deer from the Texas Panhandle. *Journal of Wildlife Diseases* 17(1): 49-56.
Peterson RL, Royal Ontario Museum Division of Zoology and Paleontology. 1952. A Review of the Living Representatives of the Genus *Alces*.
Peterson RL. 1955. North American Moose. University of Toronto Press: Toronto.
Prestwood AK, Ridgeway TR. 1972. Elaeophorosis in White-Tailed Deer of the Southeastern USA: Case Report and Distribution. *Journal of Wildlife Diseases* 8: 233-236.
Roberts LS, Janovy Jr. J, Nadler S. 2013. Phylum Nematoda: Form, Function, and Classification. In: *Foundations of Parasitology*, Schmidt GD, Roberts LS, editors. McGraw-Hill: New York, New York, pp. 349-376.
Sinclair ARE. 2003. The Role of Mammals as Ecosystem Landscapers. *Alces* 39: 161-176.

Speed JDM, Austrheim G, Hester AJ, Solberg EJ, Tremblay JP. 2013. Regional-Scale Alternation of Clear-Cut Forest Regeneration Caused by Moose Browsing. *Forest Ecology and Management* 289: 289-299.
Testa JW. 2004. Population Dynamics and Life History Trade-Offs of Moose (*Alces alces*) in South-Central Alaska. *Ecology* 85: 1439-1452.
Timmerman HR, Rodgers AR. 2017. The Status and Management of Moose in North America -- Circa 2015. *Alces* 53: 1-22.
Towbin H, Staehelin T, Gordon J. 1979. Electrophoretic Transfer of Proteins from Polyacrylamide Gels to Nitrocellulose Sheets: Procedure and Some Applications. *Proceedings of the National Academy of Sciences of the United States of America* 76(9): 4350-4354.
Wehr EE, Dikmans G. 1935. New Nematodes (Filariidae) from North American Ruminants. *Zoologischer Anzeiger* 110: 202-208.
Worley DE. 1975. Observations on Epizootiology and Distribution of *Elaeophora schneideri* in Montana Ruminants. *Journal of Wildlife Diseases* 11: 486-488.
Worley DE, Anderson CK, Greer KR. 1972. Elaeophorosis in Moose from Montana. *Journal of Wildlife Diseases* 8: 242-244.
Wunschmann A, Armien AG, Butler E, Schrage M, Stromberg B, Bender JB, Firshman AM, Carstensen M. 2015. Necropsy Findings in 62 Opportunistically Collected Free-Ranging Moose (*Alces alces*) from Minnesota, USA (2003-2013). *Journal of Wildlife Diseases* 51: 457-465.

VITA

Megan D. Miller was born in Austin, TX in 1993. Throughout her youth, she engaged in many creative activities such as painting, writing, and playing clarinet in the school band. As a high-school student, she planned to double-major in college in mechanical engineering and music education with the eventual goal of becoming a high school band director who happened to be a trained engineer. She moved to Boulder, Colorado in 2011 to attend the University of Colorado and fulfil this dream (and to climb some cool rocks). However, life has a way of changing your plans, and she changed majors several times before finding a home in the Ecology and Evolutionary Biology department. While obtaining her Bachelor's degree, she worked as an undergraduate research assistant studying the effects of ectoparasitic nest mites on the development of the immune system in nestling barn swallows (*Hirundo rustica*).

After graduating with her Bachelor's degree, she moved to Durham, North Carolina where she fell back in love with animal health while working as a veterinary assistant. However, there was a laboratory bench-shaped hole in her heart. So, when she got an opportunity to get back in the lab to study wildlife diseases and parasitology, she jumped in head first. She intends to receive her Masters of Science degree in May 2019 and continue to pursue a career in laboratory-based research.